Augmenting microbially induced carbonate precipitation of soil with the capability to self-heal

Author 1: Stefani Botusharova Ph.D. (School of Engineering, Cardiff University, Cardiff, UK)

Author 2: Diane Gardner Ph.D. (School of Engineering, Cardiff University, Cardiff, UK - ORCID number: 0000-0002-2864-9122)

Author 3: Michael Harbottle D.Phil. (School of Engineering, Cardiff University, Cardiff, UK - ORCID number: 0000-0002-6443-5340)

Corresponding author: M. Harbottle, School of Engineering, Cardiff University, Queen's Buildings, The Parade, Cardiff, CF24 3AA, UK. E: harbottlem@cardiff.ac.uk. Tel: +44 2920 875759.

Abstract

Microbially induced carbonate precipitation (MICP) is increasingly being explored as a potential ground improvement mechanism, both for improved mechanical performance and groundwater control. However, the formation of a brittle cemented monolith will produce structures susceptible to chemical or physical deterioration over time, requiring potentially costly maintenance in future. Here, we present a demonstration of the potential for a simple and durable self-healing mechanism to be incorporated within the MICP process which allows the monolith to automatically respond to and heal damage. By selecting a bacterium capable of both causing MICP and surviving long periods and harsh conditions as a spore, it is demonstrated that such an organism can be entombed within calcium carbonate precipitates of its own making, survive in a senescent state and ultimately germinate upon damage to the encapsulating precipitate matrix. Subsequently, the organism is then capable of producing further calcium carbonate to heal the damage. It has further been shown that this mechanism can be used to initially cement a mass of sand, survive damage and deterioration and respond to restore the functionality of the stabilised mass, exhibiting the potential for such a system to provide 'smart', autonomous stabilised soil structures that offer enhanced durability and reduced maintenance.

Introduction

Microbially induced carbonate precipitation (MICP) has drawn much attention for geotechnical and geoenvironmental applications, not only in ground improvement and contaminant containment (DeJong et al. 2011; DeJong et al. 2013; Ivanov and Chu 2008; Mujah et al. 2017) but also in construction materials and elsewhere (De Muynck et al. 2010; Phillips et al. 2013). Such biologically induced mineralisation in soils leads to particle cementation, pore filling and sequestration of contamination through the formation of a durable calcium carbonate mineral phase and a monolithic mass of cemented soil grains. However, over time deteriorative mechanisms will lead to a gradual breakdown of the monolith, and subsequent loss of performance (e.g. loss of bearing capacity, release of encapsulated contaminants). These mechanisms may include chemical deterioration through exposure to groundwater or physical break-up of the monolith due to external loads – both large-scale immediate and small-scale cumulative damage. However, MICP may be adapted to incorporate the potential to self-heal damage over both short and long-term timescales, leading to potentially significant enhancements in durability and therefore confidence in the technique.

In the most common application of MICP in the subsurface, a chemical reaction is triggered by microorganisms that express the urease enzyme, thus hydrolysing urea (DeJong et al. 2006). The process results in the release of ammonia and carbonate ions, which cause the pH to increase in the vicinity of the bacterial cell and precipitation of calcium carbonate to occur around the cell walls. Sufficient biomineralisation can cement sand grains together and effectively increase the strength and stiffness (DeJong et al. 2006; van Paassen et al. 2010; Whiffin et al. 2007) and enhance resistance to erosion and formation of dust (Stabnikov et al. 2011). In addition, this can significantly affect the hydraulic conductivity of the treated soil, and so has been used in applications such as sealing of reservoirs (Chu et al. 2013) or control of flow, for example in enhanced oil recovery (Ferris et al. 1996; Gollapudi et al. 1995). Carbonate biomineralisation is also valuable in encapsulating and reducing the mobility of metallic contaminants (Fujita et al. 2010; Mugwar and Harbottle 2016) and sequestering carbon dioxide (Cunningham et al. 2009; Mitchell et al. 2010).

Materials that exhibit the potential for self-healing (i.e. an ability to overcome the natural tendency for material degradation or damage over time through adaptation and response to external stimuli) offer enhanced durability, increased safety and reduced maintenance costs. They have been explored for a wide range of engineering applications (Zwaag and Schmets 2007), including cementitious construction materials (Joseph et al. 2010), where MICP or related techniques have been employed to close and heal cracks through carbonate precipitation, thereby reducing ingress of moisture and deleterious agents such as chlorides, and potentially restoring some mechanical performance (Wang et al. 2012; Wiktor and Jonkers 2011). The self-healing behaviour is brought about through the action of microbial spores, which allows populations of relevant organisms to survive long periods in a senescent state, only activating once the availability of suitable chemical precursors and a suitable environment for survival are present (both delivered through exposure to the external environment via cracking). However, challenges to the viability of this technique in cementitious materials remain due to the challenging nature of the concrete environment for microbial survival (e.g. extremely high pH, challenges to cell or spore survival due to crushing or isolation within the pore space as hydration reactions develop).

Autogenous self-healing properties (a function of natural properties) of geotechnical systems and soil structures such as fine-grained low plasticity or highly swelling soils closing fissures and cracks have been identified (Eigenbrod 2003). However, soil structures could be engineered to exhibit self-healing behaviour (an autonomous response) through adaptation of existing MICP techniques (Harbottle et al. 2014) - such environments are more welcoming than cementitious materials to such an approach as issues with pore space and chemistry are less problematic. Sand samples subjected to biocementation using *Sporosarcina pasteurii* were shown to retain their metabolic activity immediately post-mechanical damage and cause some restoration of mechanical performance after further supply of nutrients (Harbottle et al. 2014; Montoya and Dejong 2013). This was attributed to bacterial cells of *S. pasteurii* surviving the damage event and producing further mineralisation to heal the damage, however this could not be relied upon to provide a long-term, reliable self-healing response. Similarly,

work has demonstrated the potential of the ureolytic, spore-forming, *Bacillus megaterium* to bring about damage recovery to pile foundations. The bacterium together with nutrients were supplied immediately after the damage was initiated and therefore the "healing" effect may not necessarily be attributed to the spores but to still active, vegetative bacteria (Duraisamy 2016).

The following concept of self-healing MICP-treated soils is therefore explored: spores trapped within calcite are exposed by damage and germinate into cells which heal the damage, re-encapsulating themselves and resetting the cycle, as displayed graphically in Figure 1. Here we demonstrate autonomous self-healing MICP using a reliable and durable spore forming, urease-positive organism, *Sporosarcina ureae*, through the following objectives:

i. to explore the self-healing process in idealised conditions in aqueous solution, through cycles of sporulation, carbonate precipitation, and regeneration;
ii. to demonstrate the ability of the organism to bring about MICP and monolith formation;
iii. to cause monolith degradation through chemical and physical means and demonstrate spore exposure and germination;
iv. to demonstrate the ability of sporulating organisms (as opposed to less durable non-sporulating organisms) to survive the initial cementation process in spore form and in response to subsequent damage, germinate and cause healing of the damaged mineral monolith with minimal intervention.

Experimental methodology and materials

Bacterial strains and media

Sporosarcina ureae, a spore-forming, aerobic, ureolytic bacterium, was obtained from the National Collection of Industrial and Marine Bacteria, UK (NCIMB 9251). Frozen stock cultures were used to inoculate liquid growth medium, containing per litre of deionized water: 5 g peptone, 3 g meat extract, 20 g urea (filter sterilised). The pH (unadjusted) was approximately 6.5. Flasks were incubated at 30ºC at 150 rpm until an optical density at 600 nm wavelength of 0.9-1.2 was obtained (10^7-10^8

cells/ml). Cells were then centrifuged at 3200 rcf for 20 min, washed in phosphate buffered saline (PBS; 8 g NaCl, 1.42 g Na_2HPO_4, 0.24 g KH_2PO_4, per litre of deionized water, pH 7.2 - minimises osmotic stresses to the cells induced by deionised water) and centrifuged again prior to resuspension in the appropriate medium for experimentation.

Sporosarcina pasteurii (formerly known as *Bacillus pasteurii* (Yoon et al. 2001)) is a highly ureolytic, aerobic bacterium (National Collection of Industrial and Marine Bacteria, UK; NCIMB 8221). Despite the name, testing showed that this strain of *S. pasteurii* did not sporulate under a range of conditions (Botusharova 2017), and so is considered in this study as a non-sporulating organism and used as a control. It should therefore be noted that any reference herein to this being a non-sporulating organism only refers to the experiments and conditions applied within the confines of this study. Frozen stock cultures were used to inoculate liquid growth medium, containing per litre of deionised water: 13 g nutrient broth (CM0001, Oxoid, UK), and 20 g urea (filter sterilised). The pH was not adjusted and was typically around 6.5. Cells were prepared as for *S. ureae*.

The cementation medium, used for the induction of calcium carbonate precipitation by both strains, contained per litre of tap water: 3 g nutrient broth, 10 g NH_4Cl, 2.12 g $NaHCO_3$, 22.053 g $CaCl_2.2H_2O$, 20 g urea (filter sterilised), pH 6.5. For the induction of sporulation, the protocol specified by Zhang et al. (1997) was followed, which used an amended version of the medium proposed by Macdonald and Macdonald (1962). Cultures were grown until the early exponential phase when they contained between 10^7 and 10^8 viable cells per ml. They were then centrifuged and resuspended in a sporulation medium for 15 hours, which caused more than 90% of *S. ureae* cells to sporulate but had no observable effect on *S. pasteurii*. The sporulation medium contained per litre of deionised water: 2 g yeast extract, 3 g peptone, 4 g glucose (filter sterilised), 1 g K_2HPO_4, 3.238 g NH_4Cl, 0.132 g $CaCl_2.2H_2O$, 1.638 g $MgSO_4.7H_2O$, 0.112 g $MnSO_4.H_2O$, 0.001 g $FeSO_4.7H_2O$, 0.018 g $ZnSO_4.7H_2O$, 0.01 g $CuSO_4.5H_2O$, pH 8.5. The presence of spores in the cultures was determined microscopically according to the Schaeffer-Fulton spore stain procedure (Schaeffer and Fulton 1933) using a Schaeffer-Fulton spore stain kit (Sigma Aldrich, UK). The staining procedure involved the use

of malachite green and safranine solutions which dye bacterial spores green and vegetative cells red. Stained smears of bacteria/spores were examined under a 100x Nikon oil immersion lens with transmitted illumination (Nikon Eclipse LV100 microscope, Nikon Europe).

Experimental structure

Three main experiments (numbered 1-3) were carried out in this study.

Experiment 1. Demonstration of self-healing MICP cycles in aqueous solution

The aim of Experiment 1 was to demonstrate that a bacterial spore, encapsulated in carbonate precipitate in the process of bio-cementation, is able to respond to damage of the precipitate and germinate into an active cell capable of generating further carbonate precipitate. This is a demonstration of the fundamental cyclic principles of bacterial self-healing. Both *S. ureae* and *S. pasteurii* (as a non-sporulated control) were subjected to sporulation medium for 15 hours (sufficient time for the majority (>90%) of *S. ureae* cells to sporulate), then testing was carried out under three conditions, with the aim being to demonstrate that encapsulated spores (rather than vegetative cells) are able to survive harsh conditions through encapsulation and germinate upon damage. The details of these three conditions are:

i. Growth from cultures of autoclaved cells (control), to determine survivability of cells/spores alone. Fresh cultures of *S. pasteurii* and *S. ureae* (10 ml) were subjected to sporulation medium, creating non-sporulated *S. pasteurii* and sporulated *S. ureae*, prior to autoclave treatment (at 121ºC and 1.3 bar for 15 minutes). All cultures were then resuspended in 10 ml fresh growth medium and incubated at 30ºC / 150 rpm.
ii. Growth of cells from unsterilised MICP carbonate crystals (vegetative cells of the inoculated species only may remain), to determine survivability of encapsulated cells/spores. Freshly grown cells subjected to sporulation medium (as in (i)) were suspended in 10 ml cementation medium, and incubated at 30ºC / 150 rpm for 7 days. Samples of the resulting crystals were

transferred to microcentrifuge tubes, repeatedly centrifuged, washed in PBS and immersed in an ultrasonic water bath for 10-15 seconds to remove surface-associated cells/spores. To isolate the response of encapsulated cells/spores, half of the crystal samples were dissolved in 0.5 ml 0.1 M hydrochloric acid for 1-2 hours whereas the remainder were untreated and used as controls. Following this, all acid-treated and untreated samples were resuspended in 50 ml growth medium. Acid-treated crystals were not observed to affect the pH of the growth medium, due to partial neutralisation of the acid by the crystals and dilution within the medium.

iii. Growth of cells from autoclaved microbially induced calcium carbonate crystals, in order to determine the ability of encapsulated cells/spores to survive sterilisation attempts. The method was as for b), although after crystals were washed and sonicated they were subjected to autoclave treatment as described in (i) above.

After each treatment, samples were incubated at 30ºC in the respective growth medium and regularly monitored for microbial growth using optical density measurements.

Experiment 2. Self-healing in particulate media in response to chemical damage

Experiment 2 employed silica sand (d_{10}= 110 µm, d_{90}= 820 µm, C_U = 4.90, C_C = 1.43, maximum and minimum void ratios ($e_{max/min}$) = 0.829 and 0.567, G_s=2.73), which was acid washed to remove carbonates, then washed with deionised water and pH adjusted to neutral with sodium hydroxide. Prior to use, the sand was dried and sterilised by autoclaving (121ºC and 1.3 bar for 15 minutes).

This experiment explored the potential for self-healing in sand columns subject to chemical deterioration of calcium carbonate precipitate. Nine acrylic columns (inner diameter 26 mm; length 68 mm) were prepared identically, sealed with rubber stoppers and with glass wool at either end to prevent escape of sand and to minimise clogging at the inlet or outlet (Figure 2a). Sand was wet pluviated (to achieve full saturation) into one and a half pore volumes of a suspension of sporulated *S. ureae* in PBS in each column, and vibrated until a target of 95 % relative density was reached. Each column was connected to a peristaltic pump *via* ports in the stoppers, allowing the aseptic injection of

193 sterile solutions. The nine columns were divided into three triplicates and treated as follows for the
194 stages of cementation, chemical damage and healing.
195
196 Columns 1-3 were incubated at 30ºC, and subjected to an initial cementation stage, where MICP was
197 encouraged through the supply of cementation medium over a period of 29 days (5 injections of 1.5
198 pore volumes each, to ensure full displacement of existing pore fluid). An incubation period of 5-7
199 days between injections was found to be necessary for a significant amount of substrates to be
200 metabolised by *S. ureae* and converted to $CaCO_3$. Flow was maintained at 2 ml/min and was supplied
201 from the bottom of the columns. Effluent was collected for chemical analysis. Following cementation,
202 these columns were dismantled for measurement of loss on ignition (LOI) as a measure of the mass of
203 carbonate precipitated in the sand. In reality, a proportion of the mass loss would be due to the
204 presence of biomass, however, earlier experiments showed that biomass from the bacterial cell
205 suspension typically contributed only around 0.5% mass loss (results not presented).
206
207 Columns 4-6 were cemented in an identical manner to columns 1-3, but were then subjected to
208 chemical deterioration of cementation by injecting one pore volume of 0.1 M hydrochloric acid and
209 leaving for 2 hours; this was repeated three times to ensure a sufficient breakdown of the $CaCO_3$
210 matrix. The action of the acid was used to model a worst-case scenario of chemical deterioration in a
211 real environment. Higher concentrations (0.5 and 1 M HCl) were found to break down crystals more
212 effectively but limited or prevented (respectively) germination and regrowth from dissolved crystals.
213 These columns were then dismantled to determine LOI.
214
215 Columns 7-9 were treated identically to columns 4-6 but after acid treatment they were flushed with
216 two pore volumes of 0.5% hydrogen peroxide solution and left for 1-2 hours (repeated once) to kill
217 vegetative cells. This was used to model a worst-case scenario where no original vegetative cells
218 survived, to demonstrate that even in such an eventuality the system would operate. Exposure to 0.5%
219 hydrogen peroxide has been found to be effective in killing bacteria (Alfa and Jackson, 2001) whilst
220 spores of *Bacilli* and other species are able to resist even high concentrations albeit with damage

(Setlow and Setlow, 1993). We found that this concentration entirely eliminated vegetative cells in aqueous solution and in sand columns whilst spores in aqueous solution were also damaged but there was survival, particularly in association with calcite precipitates. We therefore attribute subsequent activity to germination of viable spores. Subsequently, cementation media was supplied to the columns to encourage healing through further cementation. However, difficulties were encountered in stimulating growth and so the contents of these columns were transferred aseptically to sterile flasks and incubated at 30ºC in a shaking incubator. These flasks were supplied with two pore volumes of cementation medium (replaced aseptically by pipette five times over 26 days). After this period, the LOI of the solid phase was determined.

Experiment 3. Self-healing in particulate media in response to physical damage

Experiment 3 explored the potential for self-healing in sand columns subject to physical deterioration (via mechanical damage) of the calcium carbonate precipitate. The basic preparation and operation of the sand column samples was identical to that described for Experiment 2. Experiment 3 comprised ten sand columns prepared in 0.2 mm latex rubber membranes with 3D-printed plastic discs top and bottom (diameter 38 mm; thickness 6 mm; 57 holes of 2 mm diameter), as shown in Figure 2b. These discs ensured a more uniform flow distribution across the sand specimen and minimised clogging of the inlet or outlet. A layer of glass wool around the discs prevented sand from escaping. Rubber stoppers at the inlet and outlet provided connection to the pump as before. During cementation and healing stages the columns were supported with an acrylic split mould (inner diameter 38 mm; length 68 mm) held together with zip ties.

After an initial cementation period of 38 days (7 injections), all columns were washed with deionized water, drained and air-dried to constant mass at 30ºC (approximately 3 weeks) to minimise effects of moisture on compressive behaviour whilst maintaining membrane integrity. Subsequently, the split moulds were removed and each specimen physically damaged within their latex membranes by unconfined compression testing, followed by elimination of viable cells with hydrogen peroxide as detailed for experiment 2. The sand specimens were then manually reformed into cylinders, placed

back into the split moulds for support and stored at 30ºC for the healing stage of 22 days (5 injections). The five odd-numbered columns were supplied with cementation medium whilst the remaining five even-numbered columns were supplied with deionised water. The latter acted effectively as controls without biological activity, containing only dead cells or non-germinated spores. Subsequently, the specimens were again rinsed with deionised water and air dried to constant mass, removed from their moulds and subjected to unconfined compression testing.

Analytical techniques

The effluent from column tests was filtered (0.2 µm pore size) to remove bacterial cells and precipitates. Calcium ion concentration was then determined by inductively coupled plasma optical emission spectrometry (ICP-OES; Optima 2100 DV, Perkin Elmer Inc., USA). pH was measured using a Mettler Toledo Seven Excellence pH meter (Switzerland). Optical density of 1 ml samples in 1.6 ml polystyrene cuvettes was determined at a wavelength of 600 nm using a Hitachi UV-1900 UV-visible wavelength spectrophotometer. The mass of volatile materials in sand was determined by loss on ignition (LOI), as a measure primarily of the precipitation of calcium carbonate although this would also encompass organic material such as biomass. Samples (10 g) were dried at 105ºC, weighed, then placed in a furnace at 900º C for 24 h before final weighing.

Modified falling head test

All hydraulic conductivity measurements were taken using a falling head test. Although the hydraulic conductivity was initially reasonably high, when low permeability developed a constant head test was found to be unsuitable and so for consistency a single method was used. A 6 mm diameter graduated cylinder was connected to the top of each sand column via silicone tubing just prior to each injection and used to measure hydraulic conductivity. The cylinder and tubing was filled with sterile PBS. The fluid drop with time in the cylinder was used to calculate the hydraulic conductivity of the sand specimen. Head loss in the connecting tubes was neglected (tubing length was minimised (<0.5 m)) and it was assumed that the flow retardation was only due to sand specimens.

Unconfined compressive strength test

A Stepless Compression Test Machine (Wykeham Farrance, England) was used with a 500 N capacity load cell and LVDT to measure vertical strains. Loading was performed at a rate of 1.3 mm/min (in accordance with section 7.2 of BS 1377-7: 1990 (British Standards Institution 1990)) until 20 % vertical strain. The confining effect from the membrane was subtracted as a maximum of 2 kPa at 20 % strain according to BS 1377-7: 1990, Figure 11 (British Standards Institution 1990). Measurements were taken every second using a data logger (each test was between 13 and 15 minutes in length).

Scanning Electron Microscopy

Dried calcium carbonate, produced by bacteria, was visualised using a dual beam Scanning Electron Microscope (SEM) model XB1540 (Carl Zeiss, Germany). Samples were coated with Au/Pd (80/20) using a sputter coater (Agar Scientific, Stansted, UK).

Powder X-Ray Diffraction

Oven dried samples (105 ºC) were analysed by x-ray diffraction (Phillips PW1710, Amsterdam, Netherlands) using PANalytical software (Almelo, Netherlands).

Results and discussion

Demonstration of self-healing MICP cycles in aqueous solution

Microscopic images of spore stains of sporulated and non-sporulated *S. pasteurii* and *S. ureae* cultures are shown in Figure 3. *S. pasteurii* cells appear very similar whether subjected to the sporulation medium or not (Figure 3a and b), with no spores visible either through malachite green staining or swelling of a portion of the cells. A similar lack of sporulation was observed using a range of other sporulation media (Botusharova 2017). *S. ureae* cells grown in growth medium for up to 5 hours are red due to uptake of the safranine dye only (Figure 3c), whereas cells of *S. ureae* after being exposed

to a sporulation medium for 15 hours appear dark green-blue in colour due to the uptake and retention of the malachite green dye by spores (Figure 3d).

The response of sporulated (*S. ureae*) and non-sporulated (*S. pasteurii*) organisms to autoclave treatment and carbonate precipitation was examined in Experiment 1 (Figure 4). Autoclaving served as an extreme method to remove vegetative cells, whereas in in-situ conditions this may be caused by starvation or prolonged periods of adverse environmental conditions. Neither organism demonstrated growth following autoclave treatment (Figure 4a,b), indicating that both cells and *S. ureae* spores are deactivated under this process. When precipitation of $CaCO_3$ was induced, all unsterilised carbonate crystal samples, regardless of whether they contained sporulated or non-sporulated cells, and whether or not the matrix was broken down, saw bacterial growth upon provision of growth medium (Figure 4c,d). This suggests that some cells resist the washing process as undissolved and dissolved crystals had a similar growth rate. However, with *S. ureae*, crystal dissolution led to a greater final optical density. It is unknown whether this was due to a fundamental difference in growth between *S. ureae* and *S. pasteurii*, or an indicator of increased activity due to encapsulation of both cells and spores. The short-term survival of *S. pasteurii* cells during the cementation process is likely to explain the healing effect described previously (Harbottle et al. 2014; Montoya and DeJong 2013), although in the longer term, survival of cells alone cannot be guaranteed. With autoclave-treated carbonate crystal samples (Figure 4e,f), non-sporulated *S. pasteurii* did not exhibit growth, whereas sporulated *S. ureae* did, but only when the crystals had been dissolved. The lack of growth with *S. pasteurii* demonstrates that vegetative cells did not survive the autoclaving process, whether encapsulated within the crystals or not. The survival of *S. ureae* indicates that spores survive calcification and autoclaving and demonstrate the concept of self-healing MICP - that spores encapsulated in crystals survive adverse conditions and germinate, but only upon damage to the encapsulating mineral phase. It is interesting to note that the precipitate matrix served as a protective barrier to the spores in the process of autoclaving, however this was not the case for encapsulated non-sporulated cells.

Cells regenerated from exposed spores were exposed to the cementation medium to examine their precipitation abilities after the regeneration process. The observed pH increase (Figure 5a, first cycle) in the regenerated cultures is indicative of urea hydrolysis, although the extent of the increase is weaker than that observed in ureolysis with freshly cultured cells (final pH of 8 compared to 9.2) and the variation within the replicates is larger. Crystal formation was observed and x-ray diffraction suggested that this was calcite. In contrast, pH remained unchanged in non-inoculated controls without precipitation forming. A second cycle of cell entombment in carbonate crystals, damage to these crystals and germination and growth of exposed spores was then carried out in exactly the same way using calcium carbonate precipitates created by the action of the cells germinated in the first cycle, demonstrating that the self-healing mechanism was capable of acting over at least two cycles. As shown in Figure 5a, an elevated pH response, albeit slightly weaker, was observed on this second cycle also. Crystals produced after the first cycle were observed with scanning electron microscopy (Figure 6). Conglomerations of crystals are visible, ranging from approximately 200 to 400 µm in size (Figure 6a). Large angular crystal massifs are covered in near-spherical objects (Figure 6b) which are similar in shape and size to *S. ureae* cells (see Figure 3) and so we consider these likely to be the bacteria. Rhombohedral crystals typical of calcite can be observed (Figure 6c, d), forming on and around these spherical objects. Depicted in Figure 6b is a crack formed in the mineral, which indicates that there is a rigid matrix associated with these objects.

The long-term survivability and response of spores encapsulated in calcium carbonate precipitate was explored by storing autoclave-treated MICP crystals at room temperature for 3 and 6 months. The increase in optical density observed (Figure 5b) demonstrates that spores exposed by damage to the crystal are again able to germinate and grow, albeit with a lag time increased from 20 to 30 hours, whereas undamaged crystals exhibit no such behaviour.

Self-healing in particulate media in response to chemical damage

Experiment 2 demonstrated the potential for calcium carbonate precipitation in nine identical columns (numbered 1-9) following chemical damage to an existing carbonate mineral phase. Figure 7a and c illustrate cycles of pH increase (to above 8) and calcium concentration decrease (by 90-95% apart from the last injection [average 73%]), respectively, between injection events, suggesting ureolysis and carbonate precipitation. Without urea, no such effect was observed (results not presented). This activity decreased over time, possibly due to encapsulation and limitation of nutrients to the biomass and clogging at the injection points. This relatively low activity, and the initial lack of response necessitating transfer of column specimens to flasks, may have been caused by the multiple acid and hydrogen peroxide treatments.

The initial cementation of the columns resulted in 1.6 to 1.9 % volatile material by mass of sand (columns 1-3, Figure 8). Control samples containing bacteria but not urea (results not presented) exhibited a loss on ignition of 0.85+/- 0.11% by mass (Botusharova, 2017), with approximately 0.5% attributed to biomass. This indicates that cementation produced carbonates with approximately 1% of the mass of sand (on average). During treatment with acid, 22% of this mass was lost on average (columns 4-6, Figure 8). The response of the remaining, peroxide-treated, columns 7-9 is presented in Figures 7b and d in terms of pH increase and aqueous calcium decrease, which shows a weaker response when compared to the initial cementation stage (Figures 7a and c), with the pH reaching around 8 (at the lower end of the range in Figure 7a) and the calcium decrease being around a third of that observed in Figure 7c. This indicates that microbial ureolysis was still taking place, and therefore that encapsulated organisms had survived the initial precipitation and its subsequent deterioration. On average, the pH rose above 7.7, and 9 to 42 % reduction in aqueous calcium was observed. However, a significant amount of volatile material was recovered (to up to 4 % by mass of sand - columns 7-9, Figure 8). The weakened pH and calcium conversion response at the healing stage may have been due to larger fluid volumes in the flasks diluting the observed response or may reflect the impact of acid and peroxide treatments on activity. Additionally, the acid and hydrogen peroxide treatments could

have resulted in the flushing out of spores and as no new bacteria were supplied, the metabolic potential in the sand was effectively reduced. Nevertheless, it is demonstrated that chemical damage to carbonate mineralisation is able to expose spores which germinate and resume the biomineralisation process, causing an increased precipitate mass over that present after the initial cementation.

Self-healing in particulate media in response to physical damage

Experiment 3 explored the potential for recovery of mechanical performance of sand specimens due to self-healing. In the initial cementation stage (Figure 9a and c), all specimens demonstrated a rise in alkalinity (to above pH 8.1) and removal of aqueous calcium (>90%) following each injection, similar to that observed in Experiment 2 (Figure 7). The hydraulic conductivity of the columns remained largely unchanged over the initial cementation stage, apart from columns 2 and 3, in which there was a significant drop observed (Figure 9e).

A weaker metabolic response, similar to Experiment 2, was observed in the healing stage. An average pH increase to above 7, and 30 to 58% calcium conversion can be observed in Figure 9b and d. Data from even-numbered specimens (controls) have been omitted from these figures as no change in either pH or calcium concentration was observed from that in the injected fluid. Following unconfined compression testing, the majority of columns exhibited similar values of hydraulic conductivity compared to the end of the cementation stage with the new values 67 to 122% of the previous ones (Figure 9e and f). Two columns (2 and 3) significantly decreased in hydraulic conductivity over the initial cementation stage, but upon damage these increased by factors of 2.5 and 6.5 respectively, indicating fracture of precipitates causing these low values. Over the course of the healing stage even-numbered columns treated with deionised water exhibited broadly constant hydraulic conductivity. Hydraulic conductivity was substantially reduced in all odd-numbered columns (treated with cementation medium), apart from column 7, within 22 days of healing. It was observed that column 7

had a defined diagonal shear zone formed after the first compression testing, which could have been too large for biomineralisation to block.

The results from the unconfined compression testing after both the initial cementation and healing stages are shown in Figure 10. Although a large variation in the peak strength of the 10 columns was measured (from 18 to 120 kPa), a brittle type of response with a defined peak was observed for all of the columns after the initial cementation stage (Figure 10, 'a' plots), indicative of cementation in the sand. Large peaks were observed in columns 2 and 3, reflecting the large decrease in hydraulic conductivity and showing the impacts of precipitation on both mechanical performance and flow. The hydraulic conductivity in column 7, which also exhibited a large peak strength, did not change significantly, suggesting that preferential flow paths remained around the precipitation. Columns 1 and 10 did not exhibit a defined peak in the first stage of treatment as the cementation at this stage may have been insufficient or the shear plane may have gone through an area with lower cementation. When unconfined compression testing was again performed after healing, all columns healed with cementation medium responded in a similar brittle fashion (Figure 10, odd-numbered 'b' plots), with peak strengths over and above the residual strength from the initial stress-strain curves. In contrast, all columns injected with deionised water returned to a typical, un-cemented sand behaviour, without a pronounced peak (Figure 10, even-numbered 'b' plots).

Figure 11 shows the loss on ignition from samples across each column at the end of testing, as a measure of calcium carbonate precipitation. Although a portion may be due to biomass, this would be very small (approximately 0.4 to 0.6% according to previous experimental work in the same laboratory). Typically, the mass loss from odd-numbered, treated columns with healing (1.98-2.42% on average) was greater than from treated columns without healing (1.62-1.84% on average), indicative of the additional calcium carbonate laid down in the healing stage. In the healed columns only, precipitation produced in the healing process appeared to be more prevalent at the base of the columns, nearer the inlet. There is reasonable consistency within the two treatment types in the mass loss on ignition, which correlates with the unconfined compression testing data after the healing stage.

SEM imaging shows that calcium carbonate crystals exhibited different forms and situations. Some crystals appeared to have formed in solution and were only seemingly resting on sand grains (central sand grain in Figure 12a and close up in 12b), and some which appeared to have grown as solid mass between grains, effectively providing a bond (Figure 12c). Near-spherical objects, identical to those seen in Figure 6, are clearly visible in Figure 12d, populating the surface of a carbonate crystal. Again, we consider these to be cells of *S. ureae*.

Implications of the work

The sequence of experiments presented above demonstrates that, in ideal (aqueous) conditions, ureolytic, spore-forming microorganisms such as *S. ureae* are capable of generating calcium carbonate precipitates, in which they and their spores are encapsulated, and are able to resume carbonate precipitation following regeneration upon damage to the crystalline matrix. In addition, the spores were able to remain viable for at least 6 months, and multiple cycles of sporulation, encapsulation and regeneration are possible. This demonstrates the fundamental concepts behind the self-healing process that, in principle, could be incorporated within MICP installations.

The principles were further demonstrated in Experiments 2 and 3 following both chemical and physical damage, both of which may be expected under typical conditions in the subsurface, although perhaps with less extreme conditions in many cases. The principle of self-healing may apply with any level of damage, as long as encapsulated spores are re-exposed to the wider environment. Despite an apparently slower microbial response in both experiments in the second stage, substantial extra calcium carbonate precipitation was observed, allowing for noticeable recovery of mechanical performance of damaged cemented soil specimens following the self-healing stage. We attribute the slower response and the strength gain being less than seen in the initial cementation stage to the peroxide treatment reducing the successful germination of spores. In the conditions likely to arise in reality, spores are more likely to be able to survive in large numbers.

The work presented herein is a proof of concept. Supply of ureolytic, sporulating bacteria has demonstrated the idea, and such bioaugmentation may also be employed at the field scale. However, many natural organisms possess the ability to hydrolyse urea and form spores, and other biomineralisation systems exist, and so stimulation of existing organisms is a feasible route to implementation. Both sporulation and supply of cementation media were provided in an artificial fashion to demonstrate the principles. For a truly autonomic process that does not require intervention, however, both of these need to be delivered automatically. Whilst it is entirely possible to restart the process by resupplying additional bacteria and chemicals when required, in a field setting this may be impractical (or at least inefficient) due to the difficulties involved in knowing when and where damage has occurred, delivering the new materials to the location in question, and confirming a suitable response (without considering the additional cost and effort). Sporulating organisms naturally produce spores, particularly when under environmental stress, and so artificial sporulation may not be required (it was used here to maximise numbers of spores present). For supply of cementation media, the use of microcapsules has attracted considerable attention for chemical delivery in self-healing materials and may be appropriate here (Cassidy et al. 1996; Kanellopoulos et al. 2017; Wang et al. 2014). Alternatively, many of the important requirements for cementation medium (calcium, a viable carbon source) may be naturally present at low levels in groundwater, and so ‘natural’ re-healing may be possible. There are additional factors that might impact upon the proposed system that will need to be assessed once a working system is developed. For example, access to sufficient levels of electron acceptors (oxygen, in this case) is required, although this will depend on the specific situation and even slow rates of supply *via* groundwater can be sufficient, particularly if there is not a rapid rate of continuing damage. Competition with indigenous microorganisms for chemical precursors and nutrients (once released) will take place at the edges of a precipitated mass but at damage sites within the mass the supplied microorganisms will likely dominate. Even if indigenous bacteria do act, ureolysis is still likely to take place given the widespread presence of *urease* enzymes within soil bacteria and the supply of chemicals that would support this process, and ultimately healing may be caused by both supplied and indigenous species. Further exploration is required to understand the

limitations of in-situ application, as well as the optimal method of chemical precursor/nutrient delivery.

Conclusions

It has been shown that self-healing processes can be simply introduced into microbially induced carbonate precipitation systems through the incorporation of a sporulating and carbonate-precipitating organism. The self-healing process demonstrates the potential for the system to improve the strength characteristics of soil initially, and respond automatically to chemical or physical damage by producing further calcium carbonate and restoring an element of mechanical performance. The ability of such a system to retain its viability for a prolonged period and undergo multiple cycles has also been noted. The robustness of the spores, i.e. their ability to survive under different extreme conditions imposed in the laboratory was an indication of their ability to survive various extremes in natural environments, too – these could be prolonged periods of starvation, extreme temperatures, and space confinement. The self-healing response to chemical or physical damage of the bio-cement allows adapted MICP systems to provide an effective mechanism to prevent and overcome damage to earth structures from potentially damaging processes such as erosion, low pH groundwater or applied loads, which may all cause bio-cement deterioration.

Data Availability Statement

Information on the data underpinning the results presented here, including how to access them, can be found in the Cardiff University data catalogue at https://doi.org/10.17035/d.2020.0097363828.

Acknowledgements

The authors wish to acknowledge the BRE Trust for providing the studentship of the first author. The work was carried out as part of the Materials for Life project (EPSRC Project Ref. EP/K026631/1).

References

Alfa, M. J., and Jackson, M. (2001). "A new hydrogen peroxide-based medical-device detergent with germicidal properties: Comparison with enzymatic cleaners." *Am J Infect Control*, 29(3), 168-177.

Anbu, P., Kang, C. H., Shin, Y. J., and So, J. S. (2016). "Formations of calcium carbonate minerals by bacteria and its multiple applications." *Springerplus*, 5.

Botusharova, S. P. (2017). "Self-healing geotechnical structures via microbial action." Ph.D., Cardiff University.

British Standards Institution (1990). "BS 1377 Soils for civil engineering purposes." *Part 7: Shear strength tests (total stresses)*, BSI, London, UK.

Cassidy, M. B., Lee, H., and Trevors, J. T. (1996). "Environmental applications of immobilized microbial cells: A review." *J Ind Microbiol*, 16(2), 79-101.

Chu, J., Ivanov, V., Stabnikov, V., and Li, B. (2013). "Microbial method for construction of an aquaculture pond in sand." *Geotechnique*, 63(10), 871-875.

Cunningham, A. B., Gerlach, R., Spangler, L., and Mitchell, A. C. (2009). "Microbially enhanced geologic containment of sequestered supercritical CO2." *Energy Procedia*, 1(1), 3245-3252.

De Muynck, W., De Belie, N., and Verstraete, W. (2010). "Microbial carbonate precipitation in construction materials: A review." *Ecol Eng*, 36(2), 118-136.

DeJong, J. T., Fritzges, M. B., and Nusslein, K. (2006). "Microbially induced cementation to control sand response to undrained shear." *J Geotech Geoenviron*, 132(11), 1381-1392.

DeJong, J. T., Soga, K., Banwart, S. A., Whalley, W. R., Ginn, T. R., Nelson, D. C., Mortensen, B. M., Martinez, B. C., and Barkouki, T. (2011). "Soil engineering in vivo: harnessing natural biogeochemical systems for sustainable, multi-functional engineering solutions." *J R Soc Interface*, 8(54), 1-15.

DeJong, J. T., Soga, K., Kavazanjian, E., Burns, S. E., Van Paassen, L. A., Al Qabany, A., Aydilek, A., Bang, S. S., Burbank, M., Caslake, L. F., Chen, C. Y., Cheng, X., Chu, J., Ciurli, S., Esnault-Filet, A., Fauriel, S., Hamdan, N., Hata, T., Inagaki, Y., Jefferis, S., Kuo, M., Laloui, L., Larrahondo, J., Manning, D. A. C., Martinez, B., Montoya, B. M., Nelson, D. C., Palomino, A., Renforth, P.,

Santamarina, J. C., Seagren, E. A., Tanyu, B., Tsesarsky, M., and Weaver, T. (2013). "Biogeochemical processes and geotechnical applications: progress, opportunities and challenges." *Geotechnique*, 63(4), 287-301.

Duraisamy, Y. (2016). "Strength and Stiffness Improvement of Bio-Cemented Sydney Sand." PhD, University of Sydney.

Eigenbrod, K. D. (2003). "Self-healing in fractured fine-grained soils." *Can Geotech J*, 40(2), 435-449.

Ferris, F. G., Stehmeier, L. G., Kantzas, A., and Mourits, F. M. (1996). "Bacteriogenic mineral plugging." *J Can Petrol Technol*, 35(8), 56-61.

Fujita, Y., Taylor, J. L., Wendt, L. M., Reed, D. W., and Smith, R. W. (2010). "Evaluating the Potential of Native Ureolytic Microbes To Remediate a Sr-90 Contaminated Environment." *Environ Sci Technol*, 44(19), 7652-7658.

Gollapudi, U. K., Knutson, C. L., Bang, S. S., and Islam, M. R. (1995). "A New Method for Controlling Leaching through Permeable Channels." *Chemosphere*, 30(4), 695-705.

Harbottle, M., Lam, M. T., Botusharova, S. P., and Gardner, D. R. (2014). "Self-healing soil: Biomimetic engineering of geotechnical structures to respond to damage." *7th International Congress on Environmental Geotechnics*, B. *e. al.*, ed., Engineers Australia, Melbourne, Australia, 1121-1128.

Ivanov, V., and Chu, J. (2008). "Applications of microorganisms to geotechnical engineering for bioclogging and biocementation of soil in situ." *Reviews in Environmental Science and Bio/Technology*, 7(2), 139-153.

Joseph, C., Jefferson, A. D., Isaacs, B., Lark, R., and Gardner, D. (2010). "Experimental investigation of adhesive-based self-healing of cementitious materials." *Mag Concrete Res*, 62(11), 831-843.

Kanellopoulos, A., Giannaros, P., Palmer, D., Kerr, A., and Al-Tabbaa, A. (2017). "Polymeric microcapsules with switchable mechanical properties for self-healing concrete: synthesis, characterisation and proof of concept." *Smart Mater Struct*, 26(4).

Macdonald, R.E. and Macdonald, S.W. (1962). “Physiology and Natural Relationships of Motile, Sporeforming Sarcinae.” *Can J Microbiol* 8(5) 795-808.

Mitchell, A. C., Dideriksen, K., Spangler, L. H., Cunningham, A. B., and Gerlach, R. (2010). "Microbially Enhanced Carbon Capture and Storage by Mineral-Trapping and Solubility-Trapping." *Environ Sci Technol*, 44(13), 5270-5276.

Montoya, B. M., and Dejong, J. T. (2013). "Healing of biologically induced cemented sands." *Geotech Lett*, 3, 147-151.

Mugwar, A. J., and Harbottle, M. J. (2016). "Toxicity effects on metal sequestration by microbially-induced carbonate precipitation." *Journal of Hazardous Materials*, 314, 237-248.

Mujah, D., Shahin, M. A., and Cheng, L. (2017). "State-of-the-Art Review of Biocementation by Microbially Induced Calcite Precipitation (MICP) for Soil Stabilization." *Geomicrobiol J*, 34(6), 524-537.

Phillips, A. J., Gerlach, R., Lauchnor, E., Mitchell, A. C., Cunningham, A. B., and Spangler, L. (2013). "Engineered applications of ureolytic biomineralization: a review." *Biofouling*, 29(6), 715-733.

Schaeffer, A. B., and Fulton, M. D. (1933). "A simplified method of staining endospores." *Science*, 77(1990), 194.

Setlow, B., and Setlow, P. (1993). "Binding of Small, Acid-Soluble Spore Proteins to DNA Plays a Significant Role in the Resistance of Bacillus-Subtilis Spores to Hydrogen-Peroxide." *Appl Environ Microb*, 59(10), 3418-3423.

Stabnikov, V., Naeimi, M., Ivanov, V., and Chu, J. (2011). "Formation of water-impermeable crust on sand surface using biocement." *Cement Concrete Res*, 41(11), 1143-1149.

van Paassen, L. A., Ghose, R., van der Linden, T. J. M., van der Star, W. R. L., and van Loosdrecht, M. C. M. (2010). "Quantifying Biomediated Ground Improvement by Ureolysis: Large-Scale Biogrout Experiment." *J Geotech Geoenviron*, 136(12), 1721-1728.

Wang, J. Y., Soens, H., Verstraete, W., and De Belie, N. (2014). "Self-healing concrete by use of microencapsulated bacterial spores." *Cement Concrete Res*, 56, 139-152.

Wang, J. Y., Van Tittelboom, K., De Belie, N., and Verstraete, W. (2012). "Use of silica gel or polyurethane immobilized bacteria for self-healing concrete." *Constr Build Mater*, 26(1), 532-540.

595 Whiffin, V. S., van Paassen, L. A., and Harkes, M. P. (2007). "Microbial carbonate precipitation as a
596 soil improvement technique." *Geomicrobiol J*, 24(5), 417-423.
597 Wiktor, V., and Jonkers, H. M. (2011). "Quantification of crack-healing in novel bacteria-based self-
598 healing concrete." *Cement Concrete Comp*, 33(7), 763-770.
599 Yoon, J. H., Lee, K. C., Weiss, N., Kho, Y. H., Kang, K. H., and Park, Y. H. (2001). "Sporosarcina
600 aquimarina sp nov., a bacterium isolated from seawater in Korea, and transfer of Bacillus globisporus
601 (Larkin and Stokes 1967), Bacillus psychrophilus (Nakamura 1984) and Bacillus pasteurii (Chester
602 1898) to the genus Sporosarcina as Sporosarcina globispora comb. nov., Sporosarcina psychrophila
603 comb. nov and Sporosarcina pasteurii comb. nov., and emended description of the genus
604 Sporosarcina." *Int J Syst Evol Micr*, 51, 1079-1086.
605 Zhang, L., Higgins, M. L., and Piggot, P. J. (1997). "The division during bacterial sporulation is
606 symmetrically located in Sporosarcina ureae." *Mol Microbiol*, 25(6), 1091-1098.
607 Zwaag, S. v. d., and Schmets, A. J. M. (2007). *Self healing materials : an alternative approach to 20*
608 *centuries of materials science*, Springer, Dordrecht, The Netherlands.

609 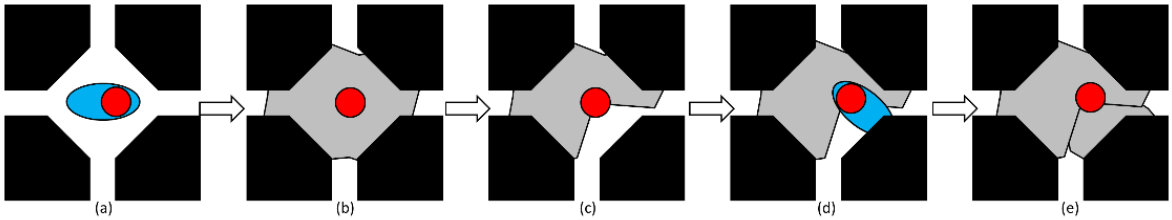

610 Figure 1. The concept of bacterial self-healing in porous media. Sporulated bacteria (a) lead to
611 mineral products within porous media containing entombed spores (b). Deterioration of the mineral
612 exposes spores (c). Germination of new cells from spores (d) causes further mineral formation and
613 new spore encapsulation (e).

614

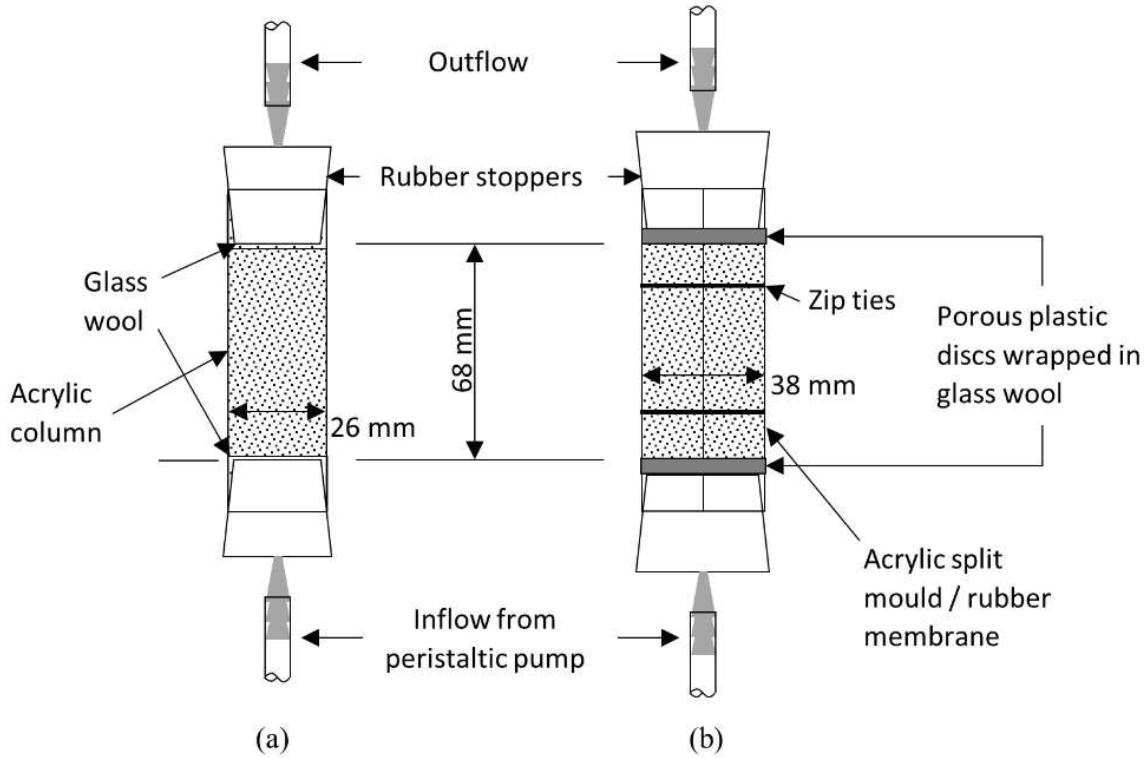

615

616 Figure 2. Testing apparatus for (a) experiment 2- sand columns for chemical deterioration experiment

617 and (b) experiment 3- split mould sand columns for physical deterioration experiment.

618

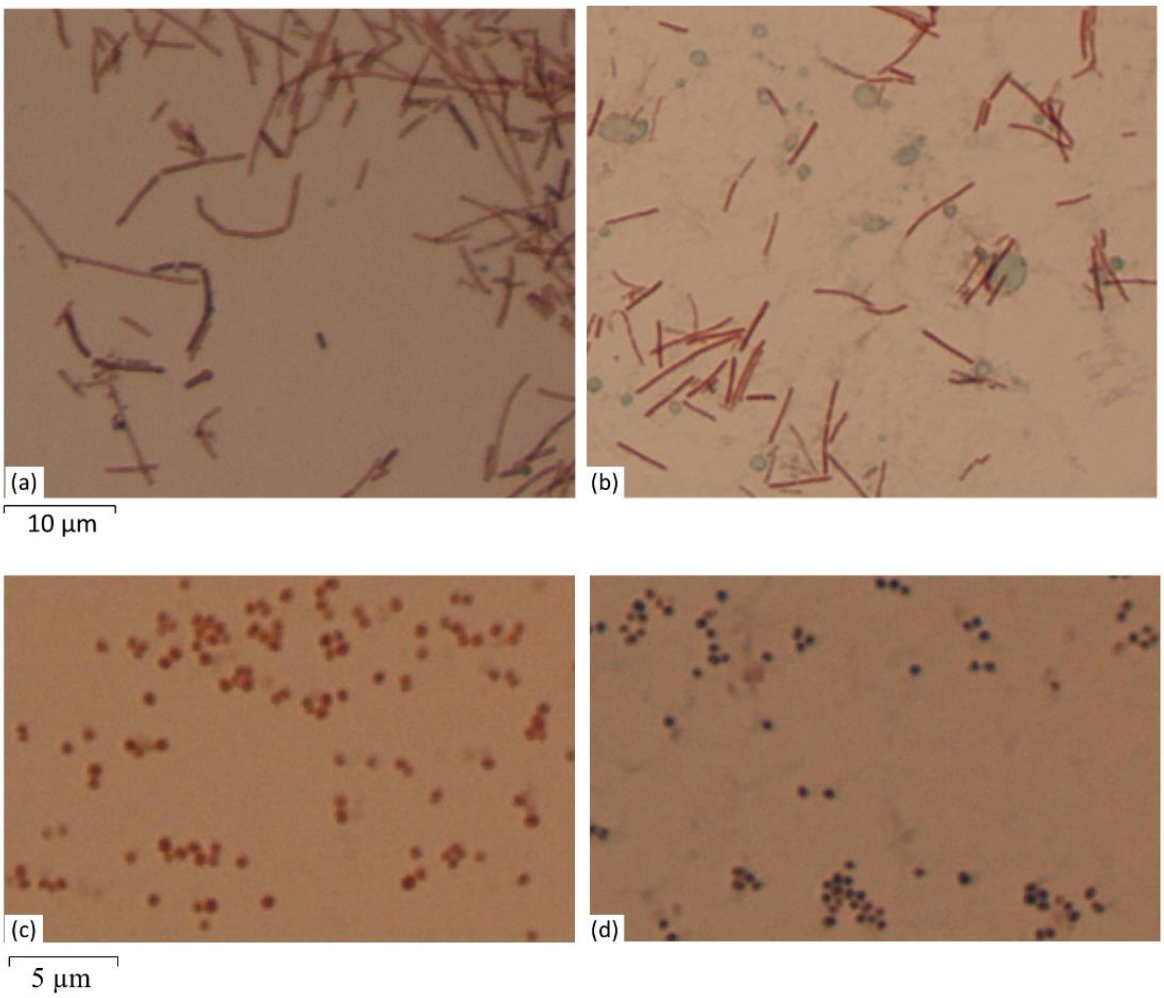

619

620 Figure 3. Schaeffer-Fulton spore staining of *S. pasteurii* (a – non-sporulated, b – subjected to

621 sporulation medium) and *S. ureae* (c – non-sporulated, d – subjected to sporulation medium) cultures.

622

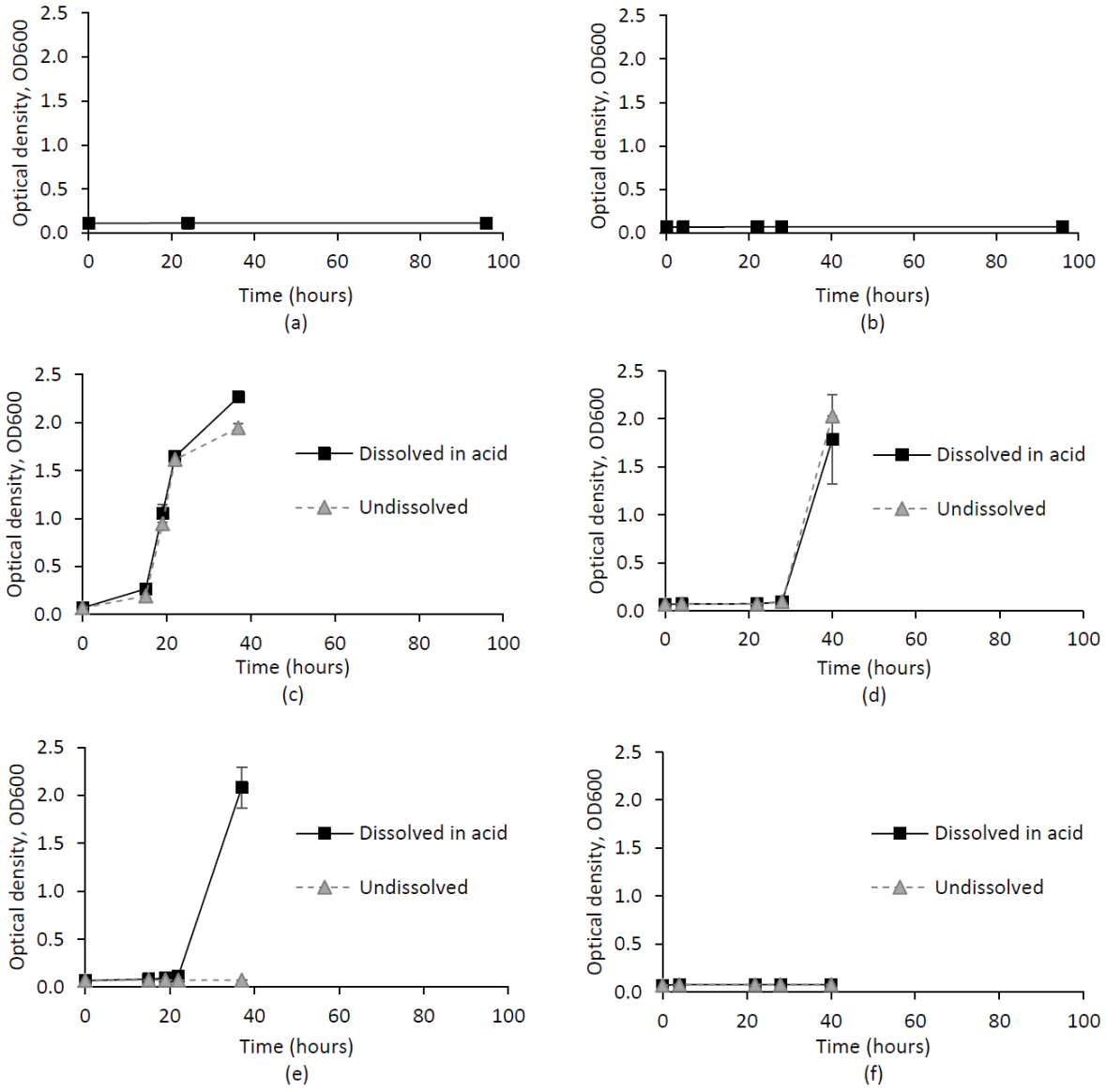

623

624 Figure 4. Experiment 1 - growth of *Sporosarcina ureae* (sporulating organism, Graphs a, c, and e) and
625 *Sporosarcina pasteurii* (non-sporulating organism under the conditions employed, Graphs b, d, and f)
626 following autoclave treatment (a and b); carbonate crystal formation (c and d) or carbonate crystal
627 formation and autoclave treatment (e and f). (Error bars: ± 1 standard deviation (SD), n=3.

628

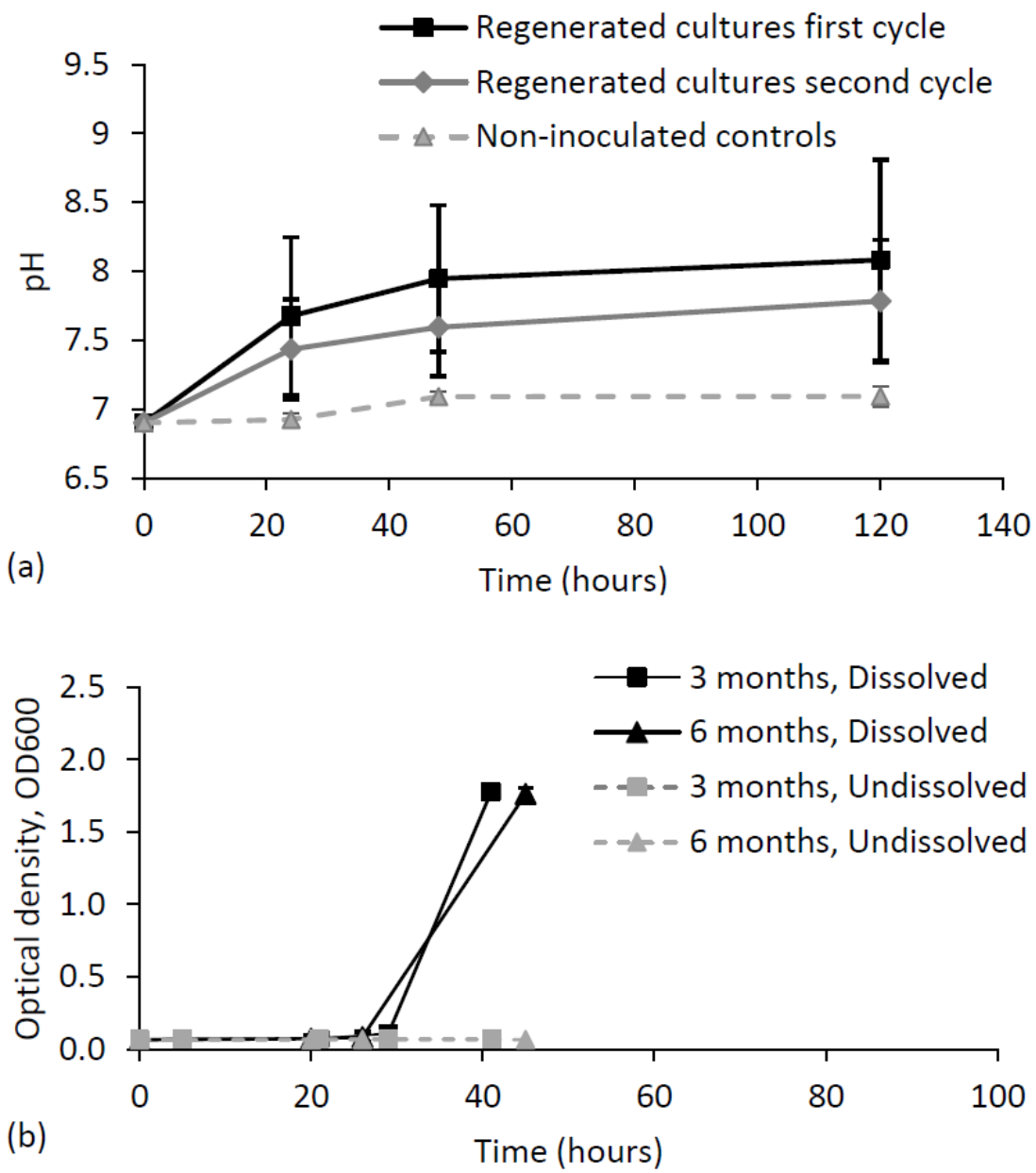

629

630 Figure 5. (a) pH increase induced by regenerated spores of *S. ureae* in cementation medium. (Error

631 bars: ±1 SD, n=5). (b) Long-term survivability of *S. ureae* spores, encapsulated in $CaCO_3$. (Error bars:

632 ± 1 SD, n=5).

633

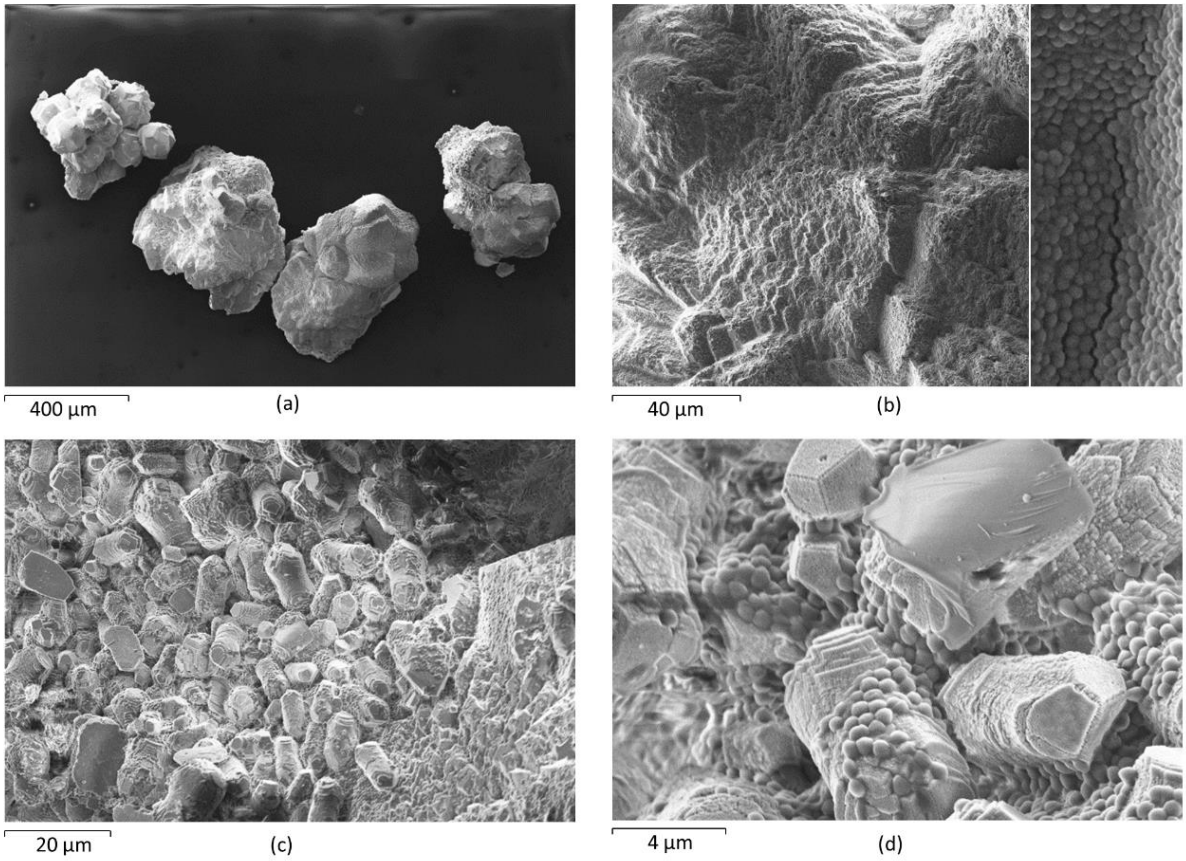

634

635 Figure 6. SEM images at increasing magnifications of $CaCO_3$ formed by *S. ureae* cells after the first
636 cycle in aqueous solution, with large conglomerations of crystals sizes between 200-400 µm (a); close
637 up of the surface of the crystals revealed either: an angular massif of calcium carbonate covered in
638 spherical objects similar to cocci bacteria (b), or small 10-15 µm hexagonal, cylindrical crystals,
639 forming a conglomeration (c, d).

640

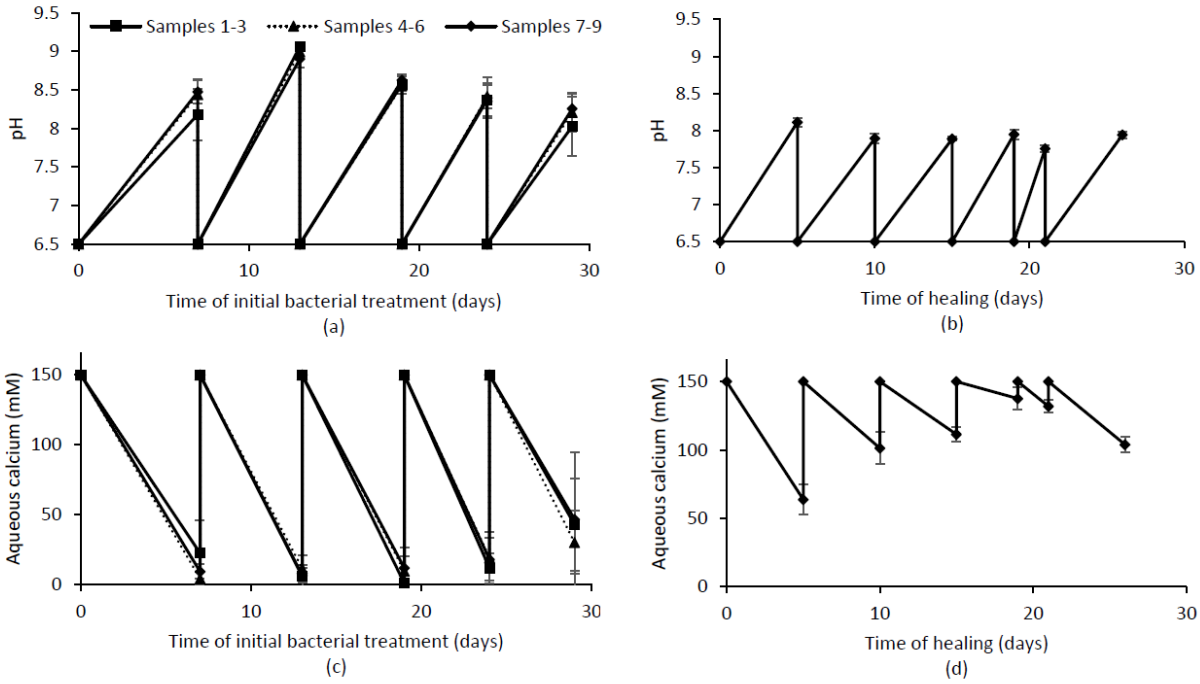

641

642 Figure 7. pH (a, b) and aqueous calcium concentration (c, d) in initial cementation (a, c) and healing

643 (b, d) stages (columns 7-9 only) in Experiment 2.

644

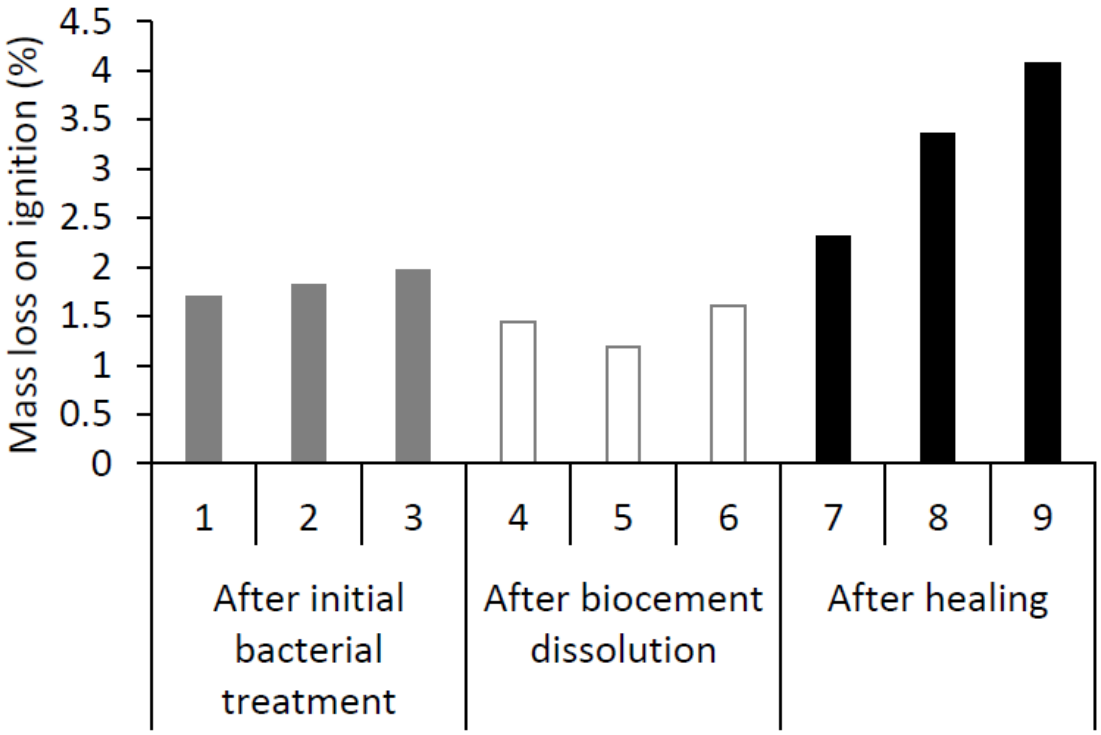

645

646 Figure 8. Mass of $CaCO_3$ initially formed (columns 1-3); mass of $CaCO_3$ present after acid dissolution

647 (columns 4-6); mass of $CaCO_3$ present after healing stage (columns 7-9).

648

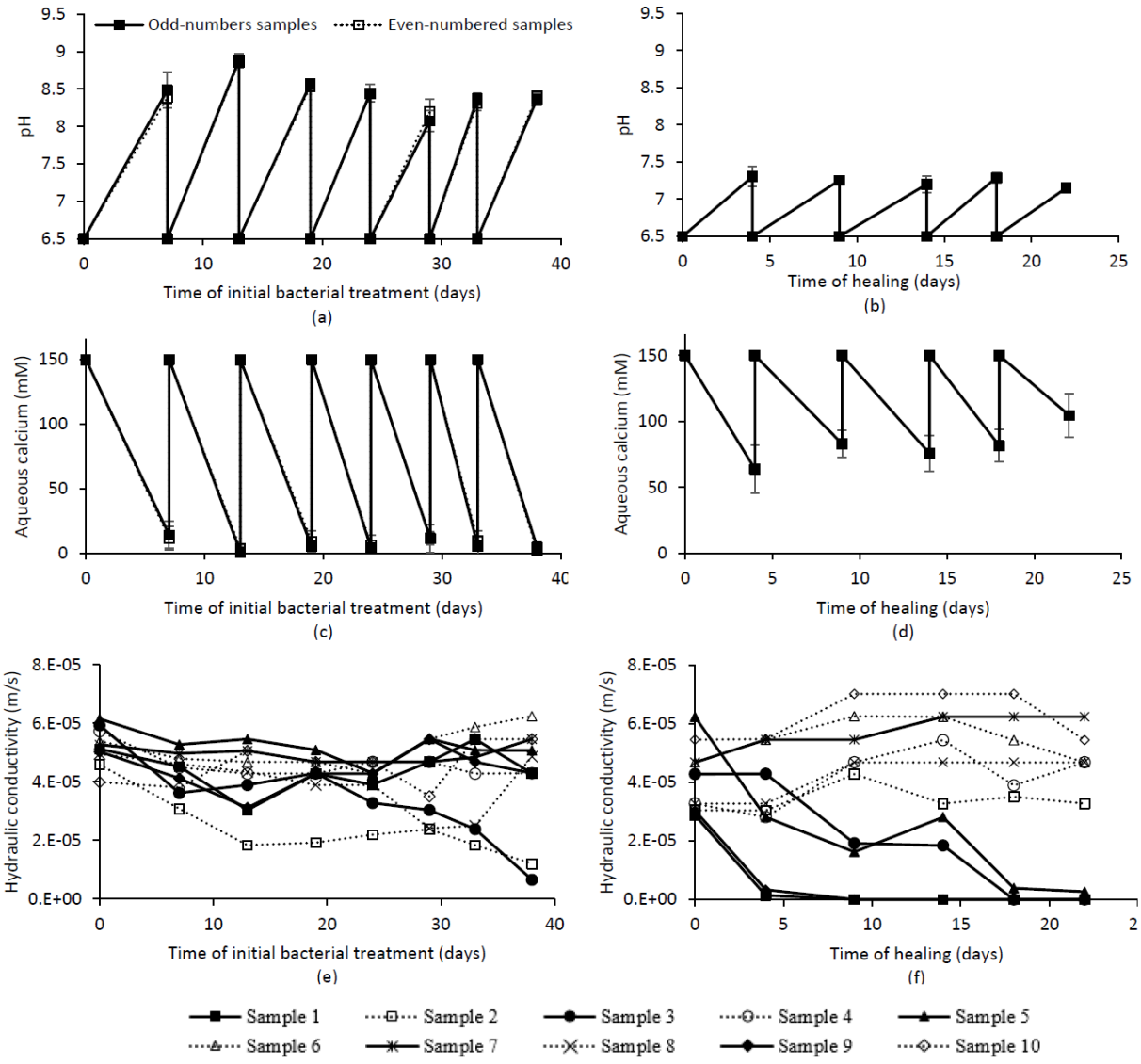

649

650 Figure 9. pH (a, b), aqueous calcium concentration (c, d) and hydraulic conductivity (e, f) in initial
651 cementation (a, c, e) and healing (b, d, f) stages in Experiment 3. All 10 columns were initially
652 bacterially cemented; after physical deterioration (unconfined compression), odd-numbered
653 specimens were injected with nutrients and even-numbered specimens were injected with deionized
654 water. Data from even-numbered specimens are not presented on figures b and d (no effect observed).

655

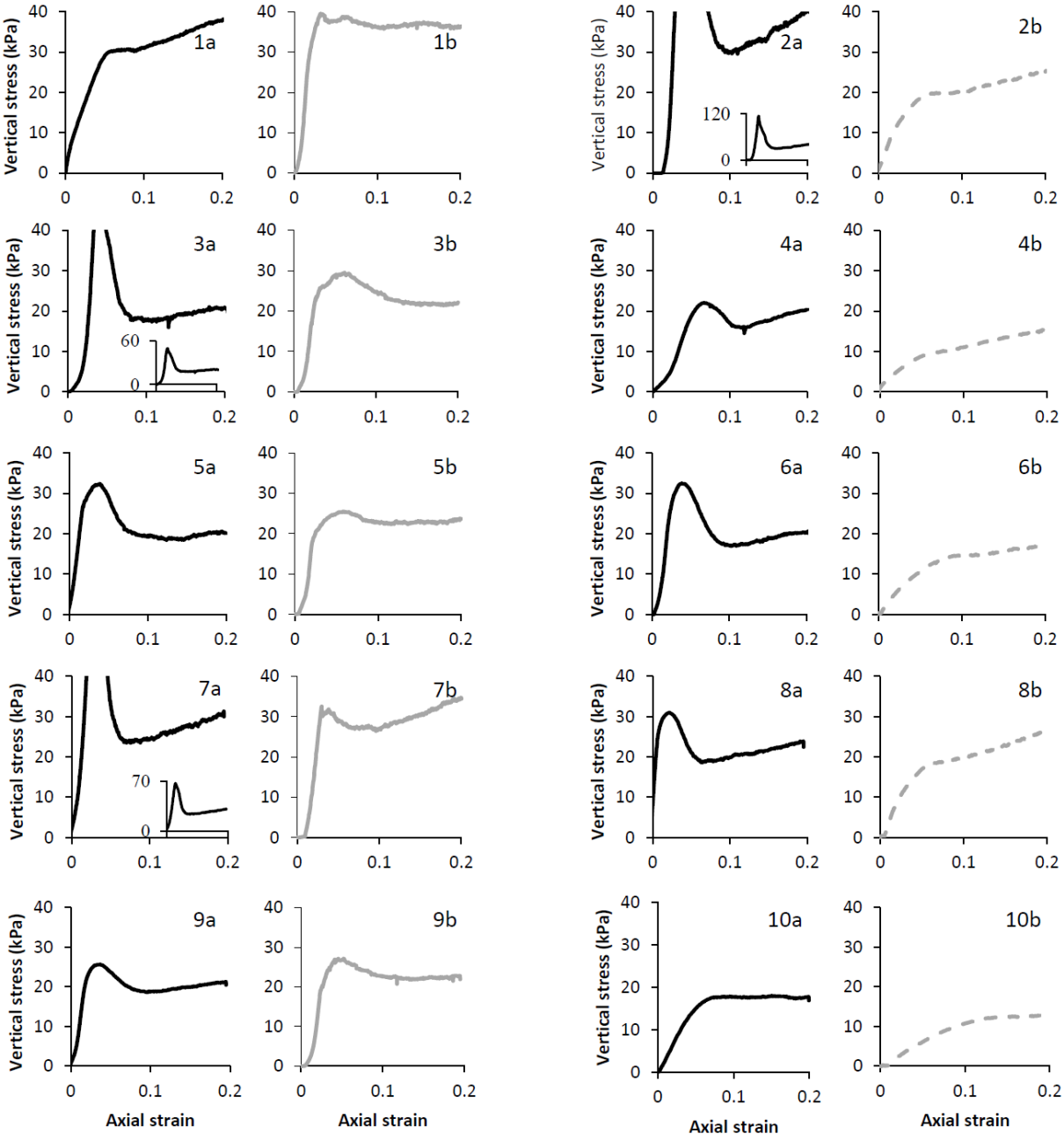

Figure 10. Unconfined compression after the initial cementation ('a' plots) and healing stages ('b' plots) of sand specimens. Odd-numbered specimens were injected with cementation medium at the healing stage, whereas even-numbered specimens were injected with deionised water.

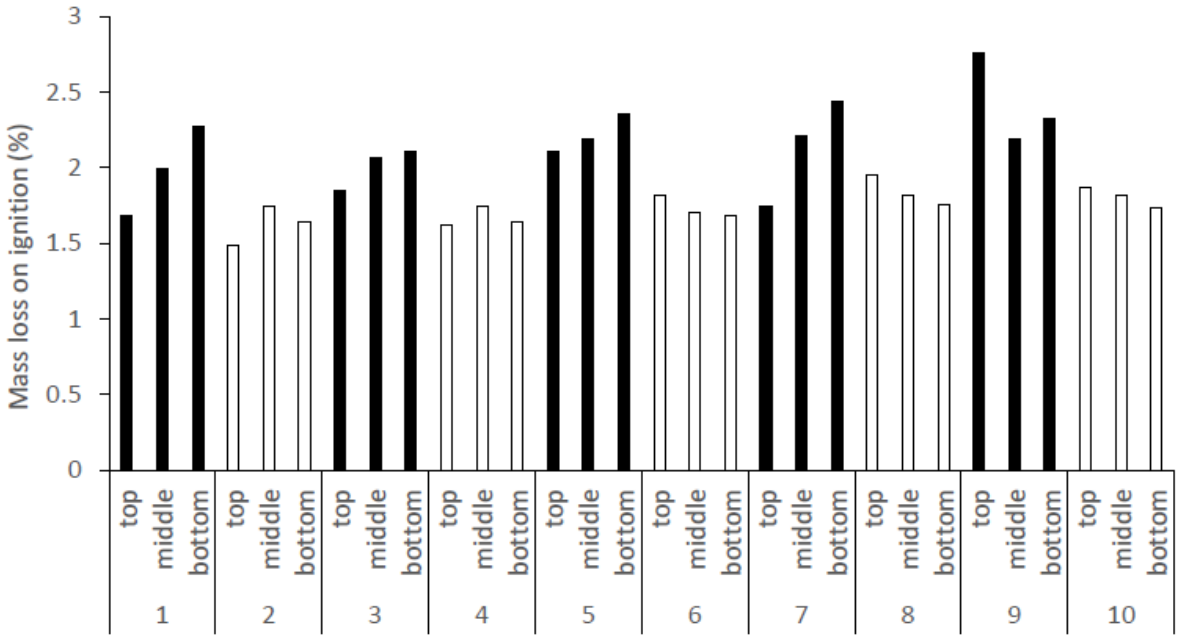

661

662 Figure 11. Loss on ignition as a measure of the amount of calcium carbonate precipitated in sand

663 columns at end of experiment. Odd-numbered specimens were injected with cementation medium at

664 the healing stage, whereas even-numbered specimens were injected with deionised water.

665

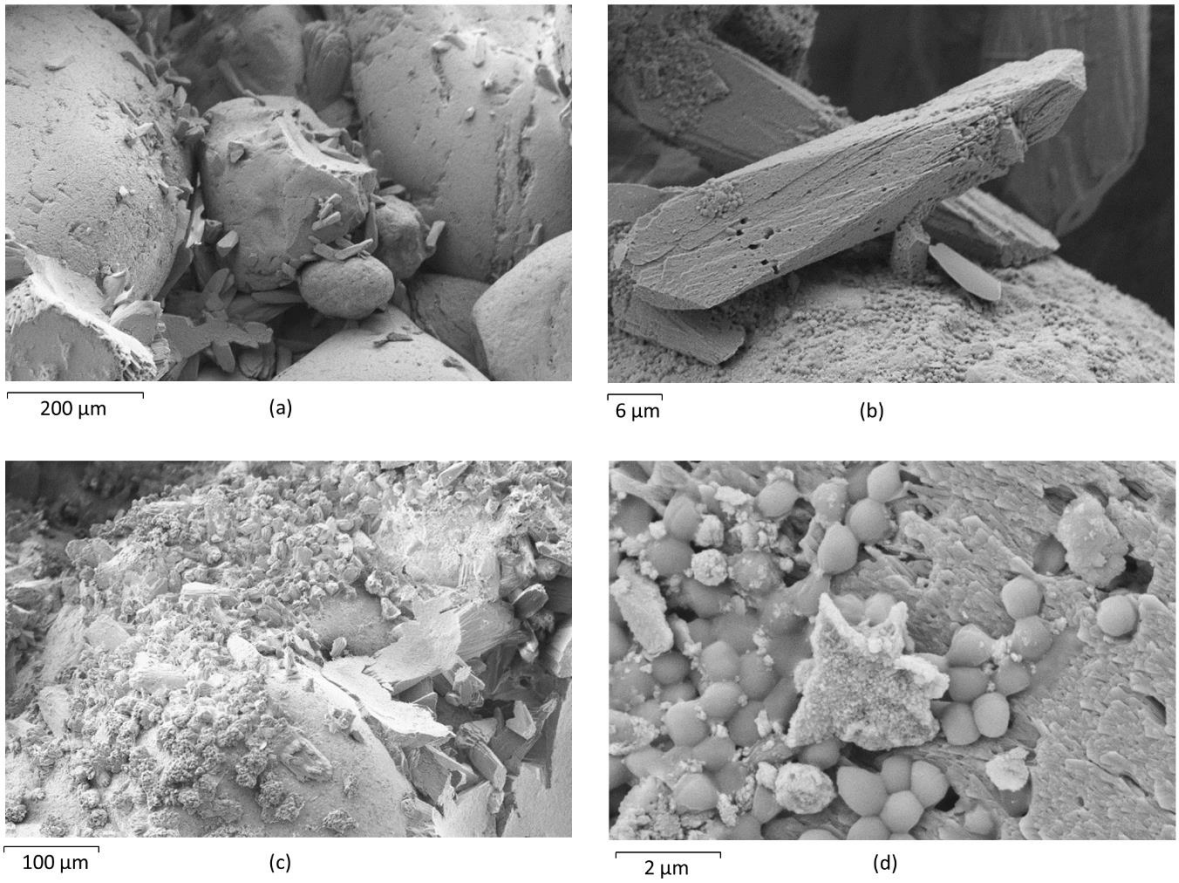

666

667 Figure 12. SEM images of $CaCO_3$ formed by *S. ureae* within sand. Crystallisation appeared to have
668 occurred in two ways: precipitates formed in the pore space and only "resting" on sand grains (a) and
669 (b), and solid mass of calcium carbonate growing in-between sand grains, almost fully covering and
670 bonding them together (c) and close-up (d).

671